NIRS

HIMAC

NIRS-M-101
HIMAC-007

Proceedings of the Yayoi Symposium on

Ion-Beam Radiation Chemistry

弥生研究会：原子力における放射線効果（2）

ーイオンビームム放射線化学の新展開ー

Edited by Y. Katsumura
T. Murakami
Y. Yoshida

January 21, 1994

National Institute of Radiological Sciences

9-1, Anagawa 4-Chome, Inage-ku, Chiba-shi 263 JAPAN

まえがき

近年になり原研高崎のＴＩＡＲＡイオン照射施設をはじめとした様々のイオン加速器が国内でも稼働し、利用できるようになりました。さらに、平成５年の秋には千葉市にございます放射線医学研究所のＨＩＭＡＣ(Heavy Ion Medical Accelerator in Chiba)も稼働を開始しました。放射線化学研究者にとりましても、これまでの低ＬＥＴ放射線を中心とした研究から、種々のイオンを用いた高ＬＥＴ放射線化学の研究もできるようになってきております。発生できるビームの種類、エネルギーも多岐にわたり、こういったバラエティーに富んだビームを利用できる環境は世界ひろしと言えども、現在、日本以外にはないと思われます。こういったイオンビームを活用した新しい放射線化学も期待されますし、すでに幾つかのグループでは精力的にイオンビームを用いた研究課題に取り組んでおられます。こういった現状を踏まえ、平成６年１月２１日、ＨＩＭＡＣ施設のある放射線医学研究所におきまして、イオンビーム放射線化学と題しました研究会を開催することが出来ました。研究会ではＨＩＭＡＣ施設の見学をするとともに、イオンビーム放射線化学の最新の成果を聞きながら、放射線化学、放射線生物、放射線物理との接点を探り、研究グループ間の情報交換や貴重な装置の有効利用が検討できましたことは研究会の幹事として望外の喜びであります。

本報告書は、研究会で紹介頂いたご講演を記録したものです。今後、ＨＩＭＡＣを利用したイオンビーム科学の発展と、国内のこの分野の研究の進展に少しでも寄与できれば幸いです。なお、本研究会は東京大学原子力工学研究施設の弥生研究会の活動、「原子力における放射線効果（２）」として行われたことを申し添えておきます。

最後に、本研究会を開催するに当たり、放射線医学総合研究所の関係者には会場の準備、見学、懇親会にと多大な援助を頂きましたことにお礼を申し上げるとともに、ご多忙中にもかかわらず研究会に参加頂いた、講演者、参加者に深く感謝いたします。

平成6年1月23日

研究会幹事
勝村庸介　（東大工）
村上　健　（放医研）
吉田陽一（阪大産研）

参加者リスト

氏名	所属	住所
相馬純吉	神奈川大学理学部	〒 259-02 平塚市土屋 2946
峯岸安津子	同上	
三好憲雄	福井医科大学・病理学（1）	〒 910-11 福井県吉田郡松岡町下合目 23-3
浜　義昌	早稲田大学理工学総合センター	〒 169 新宿区大久保 3-4-1
木村一宇	理化学研究所・反応物理化学	〒 351 和光市広沢 2-1
今井正彦	東京都立アイソトープ総合研究所	〒 158 世田谷区深沢 2-11-1
岡田重文	原子力システム懇話会	〒 105 港区新橋 2-13-6
松尾　崇	東京医科歯科大学・難研	〒 113 文京区湯島 1-5-45
村上　健	放射線総合医学研究所	〒 260 千葉市稲毛区穴川 4-9-1
高田栄一	同上	
鷲尾方一	住友重機械工業（株）	〒 254 平塚市夕陽ケ丘 63-30
田川精一	大阪大学産業科学研究所	〒 567 大阪府茨木市美穂ケ丘 8-1
吉田陽一	同上	
田中隆一	日本子力研究所・高崎研	〒 370-12 高崎市綿貫町 1233
瀬口忠男	同上	
石井保行	同上	
南波秀樹	同上	
大野新一	同上	
山下栄一	同上	
渡辺　宏	同上	
沖垣成保	（財）癌研究会癌研究所・物理	〒 170 豊島区上池袋 1-37-1
小泉　均	北海道大学工学部	〒 060 札幌市北区北 13 西 8
富田裕之	東京大学医学部放射線管理学教室	〒 113 文京区本郷 7-3-1
柴田裕実	東京大学原子力総合センター	〒 319-11 茨城県那珂郡東海村白方白根 2-22
古澤孝弘	東京大学工学部原子力工学研究施設	〒 319-11 茨城県那珂郡東海村白方白根 2-22
浅井圭介	東京大学工学部システム量子	〒 113 文京区本郷 7-3-1
勝村庸介	同上	
堂前雅史	同上	
広石大介	同上	
松浦千尋	同上	
V.M.Byakov	同上	

from Institute for Theoretical and Experimantal Physics, Moscow, Russia

弥生研究会：原子力における放射線効果（２）
－イオンビーム放射線化学の新展開－

日時：平成６年１月２１日（金） 9:50 -
場所：放射線医学総合研究所第一会議室　〒２６３ 千葉市稲毛区穴川４－９－１

プログラム（20 分講演 + 10 分質疑）

9:50 - 10:00　開会の挨拶　（放医研　平尾泰男）

10:00 - 10:30
　原研高崎ＴＩＡＲＡの概要と研究利用　（原研高崎　田中隆一）
10:30 - 11:00
　高分子材料のイオン照射効果　（原研高崎　瀬口忠男）
11:00 - 11:30
　高分子照射効果のミクロ構造の研究　（早大理工　浜　義昌）
11:30 - 12:00
　ＨＩＭＡＣ紹介　（放医研 村上　健）
12:00 - 13:00
　ＨＩＭＡＣ施設見学

13:00 - 14:00　－－ 昼休み －－

14:00 - 14:30
　アラニンラジカル生成のイオンビーム依存性　（北大工　小泉　均）
14:30 - 15:00
　ポリシランのイオン照射効果　（阪大産研　田川精一）
15:00 - 15:30
　トラック深さ差分励起状態ダイナミクスとイオンの高密度励起効果　（理研　木村一宇）

15:30 - 16:00　－－コーヒーブレイク－－

16:00 - 16:30
　特別講演　（原子力システム研究懇話会
　　生物研究者から見た放射線化学への期待　岡田重文）
16:30 - 16:50
　ＨＩＭＡＣを用いた研究計画 Ⅰ　（阪大産研　吉田陽一）
16:50 - 17:10
　ＨＩＭＡＣを用いた研究計画 Ⅱ　（東大工　勝村庸介）
17:10 - 18:00
　フリーディスカッション　コメンター
（東京医科歯科大学　松尾　崇）
（原研高崎　渡辺　宏）

18:00　－－ 懇親会 －－

JAERI TIARA FACILITIES AND THEIR APPLICATION

R. Tanaka
Department of Advanced Radiation Technology
Japan Atomic Energy Research Institute
Takasaki, Gunma,

Abstract

The TIARA (Takasaki Ion Accelertors for Advanced Radiation Application) has been constructed from 1987 to 1993 at JAERI, Takasaki, for research and development of materials science and biotechnology. The paper outlines the present status of TIARA with our initial experience and some recent progress.

The TIARA (Takasaki Ion Accelertors for Advanced Radiation Application) facilities have been constructed from 1987 at JAERI, Takasaki, for research and development of materials science and biotechnology[1]. The TIARA consists of an AVF cyclotron (K=110), a 3 MV Tandem accelerator, a 3 MV single-ended accelerator, 400 kV ion implantor, and various experimental apparatus. The first two were completed in 1991, and have been operated for experiments[2]. The last two and their multiple beam lines were newly completed in July, 1993[3]. The full operation of TIARA for experiments started at the beginning of 1994. The specification of the TIARA is summarized in Table 1.

The JAERI AVF cyclotron is of the model 930 of Sumitomo Heavy Industries, Ltd.[4]. The two ion sources of ECR and multi-cusp types have been smoothly operated without any serious trouble. The cyclotron has been operated since January, 1992, and the weekly continuous operation from Monday to Friday started in September 1992[6]. It has worked for about 4100 hours from April 1991 to December 1993. The beam acceleration test has been tried for H(10 - 90 MeV), D(20 - 50 MeV), He(20 - 100 MeV), C(220 MeV), Ne(120, 260 MeV), Ar(175 - 460 MeV), Kr(520 MeV) ions. The beam transmission efficiency between two points just before injection and just after extraction is 8.7 % on the average. Recently it amounts up to 10 - 15 %. The yearly operation time is divided into 3 beam-time periods, each consisting of 11 to 13 weeks of beam times which are allocated in the TIARA Program Committee.

To extract pulse beams with a variety of pulse interval, the cycrotron system is equiped with a couple of beam chopping systems: a pulse-voltage chopper installed in the injection line and a sinusoidal-voltage one installed after the exit of the cycrotron. The single pulse extraction was made from a beam pulse train after the cyclotron over a wide range of energy

Table 1 Accelerator specification of TIARA

Accelerators	Ion particle	Acceleration energy (MeV)	Beam current (μA)
AVF Cyclotron	p	5 - 90	30
	d	5 - 53	40
	He	10 - 100	20
	C	30 - 330	5
	Ne	50 - 550	5
	Ar	100 - 700	5
	Kr	200 - 630	1
	Xe	310 - 620	0.1
3 MV Tandem Accelerator	p	0.8 - 6.0	5
	C	0.8 - 15.0	10
	Ni	0.8 - 15.0	5
	Au	0.8 - 9.0	15
3 MV Single-Ended Accelerator	p	0.4 - 3.0	100
	d	0.4 - 3.0	70
	He	0.4 - 3.0	70
	e^-	0.4 - 3.0	50
400 kV Ion Implanter	He	0.01 - 0.4	30
	Ni	0.01 - 0.4	30
	Au	0.01 - 0.4	30

a wide variety of ion species by using the chopper systems[5].

The cyclotron beam is two-dimensionally scanned by using a pair of deflection magnets over a wide area up to 100 x 100 mm^2 for uniform and high-anergy beam irradiation to materials and semiconductor devices. The horizontal scanning frequency is 50 Hz and the vertical one is 0.5 - 5.0 Hz. A real-time fluence-rate mapping system and an integrated dosimetric method are now under development to ensure two-dimensional uniformity over the irradiated area.

To diversify available species and the energy range of accelerated ions, we designed a new ECR ion sources with high performance of generating highly charged ions and metallic ions[7]. The highest commercially available microwave frequency of 18 GHz was chosen for the RF source for its application to $2\omega ce$ mode operation in use of room temperature magnets.

A monoenergetic neutron source has been built for accumulating basic data of radiation production by energetic ion beams, nuclear reactions of high-energy neutrons, activation cross sections and shielding. The beam is produced by ^{7}Li(p,n) reaction for 20 to 90 proton beams with variable thickness of Li targets, and transported to an experimental room through a

thick shielding wall.

The 3 MV single-ended accelerator manifactured by Nissin High Voltage Co. was designed to require an extremely high voltage-stability of $\pm 1 \times 10^{-5}$ to provide a submicron microbeam stably[3]. A balanced type Schenkel DC power supply was selected for the high voltage generator. The terminal voltage is monitored by precision voltage measuring resistirs. We are aiming at the voltage stability of $\pm 1 \times 10^{-5}$ including voltage ripple and drift. An accelerated beam is analyzed by a 90° bending magnet with a radius of 1.5 m and the energy resolution of $\pm 1 \times 10^{-5}$.

There are five beam lines: two beams for multiple beam courses, one for the submicron microbeam course, and one for electron beam course. For electron beam acceleration, the polarity of the terminal voltage can be changed to negative by reversing the polarity of diodes. The triple beam target chamber is installed for the basic study of radiation damage of various materials of nuclear fusion reactors induced by high-energy neutrons, giving rise to atomic displacement damage by recoil atoms and production of hydrogen and helium atoms by transmutation reactions. Simultaneous irradiation of a heavy ion beam and the both light beams allows the simulation of the above irradiation environment.

Two dual-beam analysis systems was designed for in-situ or successive analysis of materials surface modified by ion beams. The one connected with the tandem and implanter beam lines is to be used mainly for nuclear reaction analysis (ERDA) using heavy ions from the tandem machine. The other connected with the single-ended and implanter beam lines is to be used mainly for Ratherford backscattering (RBS) and high-resolution nuclear resonance reaction analyses using light ions from the single-ended machines.

An integrated 400 KV analytical electron microscope combined with electron and X-ray analyzers is installed at a beam line at an angle of 50° with the horizontal line from the implanter. It was designed to permit in-situ observation of dynamic process of the structural change in materials under simultaneous irradiation of beams.

Ion microbeams is the most characteristic beam application in TIARA. An emphasis is put on developing high-energy heavy-ion microbeams for studies of single event upsets (SEU) of integrated circuits and biotechnology such as cell surgery[8].

A heavy ion microbeam apparatus connected with the tandem accelerator has been developed for analysis of SEU of LSI memories in spacecrafts[9]. We achieved a beam spot size of 1 μm by using 15 MeV Ni ions. The SEU study on n-type silicon diodes was started with the measurement of single-event current transients induced by 15 MeV Nickel and Carbon ion microbeams. It is

required for SEU analysis that a high-energy single ion strikes a selected area without any previous ion hit on the area of interest. Detection of a single ion hitting and control of the hit number are being developed to realize accurate single ion hit at an aimed local sensitive area of a microcircuit.

A light ion microbeam apparatus connected with the single-ended accelerator is now under construction. To achieve a submicron beam spot size within 0.5 um, we selected the accelerator design within a voltage stability of $\pm 1 \times 10^{-5}$. This system will be applied to high-resolution analysis of implanted or deposited materials, SEU of integrated circuits and other various samples.

Higher-energy heavy ions and a single ion hit or a predetermined number of hits are needed mainly in irradiation of a preselected area of a single cell for study of cell surgery techniques, and in irradiation of whole single cell or a small organ. A sufficient requirement is that it passes through a cell or an organ, because each particle, after passing through, has to be detected for hit verification.

To conduct experiments using TIARA facilities, experimental apparatus, target chambers, and various instruments have been designed, constructed and assembled. A large number of them have been connected with beam lines from the four accelerators, and are now being used for beam experiments. Other several apparatus and chambers will be also installed at the beam course ends of the electrostatic accelerators newly constructed till the end of FY 1993.

References

1) S.Sato, in Proc. of Intern. Conf. on Evolution in Beam Application, Takasaki 1991, p239-244.
2) The JAERI TIARA Anual Report No.1, 1992 & No.2, 1993
3) Y.Saitoh, Nucl. Instr. and Meth., B, 1993, to be published.
4) K.Arakawa, et al., in Proc. of 13th Intern. Conf. on Cyclotrons and Their Applications, 1992, p119-122
5) W.Yokota, et al., ibid., p581-584
6) K.Arakawa, et al., in Proc. of 9th Symp. on Accelerator Science and Technology, Japan, 1993, p202-204
7) W.Yokota, et al., ibid.,
8) R.Tanaka, et al., Nucl. Instr. and Meth., B79, 1993, 432-435
9) T.Kamiya, et al., Nucl. Instr. and Meth., B62, 1991, 362-365

ION IRRADIATION EFFECTS ON POLYMER MATERIALS

Tadao SEGUCHI, Hisaaki KUDOH, and Tsuneo SASUGA
Department of Material Development, JAERI Takasaki

ABSTRACT

The radiation resistance of polymer materials were studied by high energy proton and helium ion irradiation. The changes of the mechanical properties and chemical reactions induced in polymers were compared with those induced by electron beam irradiation. The changes of mechanical properties for aliphatic polymers were almost same between ions and electrons when the dose absorbed in polymers was normalized, but those for several aromatic polymers were different.

INTRODUCTION

For selection and application of polymer materials used in the radiation field such as space or fusion reactor, the degradation of the materials in the environment must be evaluated. The radiation resistance of polymer materials has been studied by gamma-rays and electron beam irradiation. However, the data of ion irradiation on practical properties was very few[1-3]. The effect by ion irradiation has been thought to be different from the electron irradiation, because the linear energy transfer(LET) is much different between ion and electron. Therefore, the degradation behavior would be affected by the LET of radiation sources.

The ion irradiation chamber[4] for polymer films to irradiate uniformly on the wide area was prepared in TIARA facility in JAERI Takasaki Establishment. For several polymer materials, the changes in chemical structure and in mechanical properties were studied by proton (10 and 45MeV) and He ion(50MeV) irradiations, and compared with those induced by 2 MeV electrons irradiation.

EXPERIMENTAL

Polymers were polyethylene(PE, medium density), polytetrafluoroethylene (PTFE), polymethylmethacrylate(PMMA), polyethersulphone(PES), and bisphenol-A type polysulphone(U-PS). These polymers except PMMA(3mm) were film with about 0.1 mm thickness.

Ions were H^+(10, and 45MeV) and He^{2+}(50MeV) form AVF cyclotron accelerator. The ion irradiation was carried out by scanning the spot beam (about 10 mm diameter) in the area of 100 mm x 100 mm, with a 50Hz in horizontal and 0.2Hz in perpendicular direction. The ion current was 50 - 500 nA. The penetration depth of 10 MeV proton and 50 MeV He ion into polymer film is 110 and 170 mg/cm^2, respectively. Electron irradiation was carried out under vacuum at room temperature by scanning electron beams from a Dynamitoron 2 MeV accelerator, and the penetration depth is 0.8 g/cm^2.

The absorbed dose into polymer film by ion and electron irradiation was measured by a cellulose tri-acetate (CTA) film dosimeter. On the other hand, the absorbed dose(D) is given by;

$$D(kGy) = S(MeV\ cm^2/g) \times Q(10^{-6}C/cm^2)$$

where S is the mass stopping power of polymer material and Q is the fluence. The stopping power was calculated using Bethe's equation[5] for ions and Seltzer and Berger method[6] for electrons, and are listed in Table 1 for several polymers. The stopping power is closely related to LET.

Radiation effects were evaluated by measuring tensile properties, DSC thermograms (enthalpy of melting, glass transition temperature, molecular weight), and gel fraction.

RESULTS AND DISCUSSION

Figure 1 shows the changes of elongation at break and tensile strength measured by tensile test for polyethylene film after irradiation by ions of H^+ and He^{2+} and electrons. The dose is based on the CTA dosimeter, which is irradiated in the same condition with polymer specimens. The changes of mechanical properties are almost same between ion and electron irradiations. For PTFE film, the mechanical properties decayed with same behavior on dose by ion and electron irradiation, and also the decrease of molecular weight determined from enthalpy of crystallization with DSC thermograms was the same against dose for ions and electron irradiations. The degradation of PMMA which was determined by flexual strength with the specimen of 3 mm thick sheet was same between H^+(45MeV) and 2MeV electron.

Figure 2 shows the changes of mechanical properties for polyethersulphone (PES) film after irradiation H^+(10MeV) and electron.
The change of elongation is very different and also the tensile strength is different between ion and electron. The decaying curves of elongation and strength cross each other at dose around 0.7MGy, which means the degradation by ion irradiation become small at higher doses. For U-PS, the changes of mechanical properties were the same behavior with PES in Fig.2.

In the chemical reaction as crosslinking and main chain scission, PES and U-PS showed the different behavior between ion and electron irradiation. The one evidence was the gel formation by crosslinking; the gel fraction increases in the case of ion irradiation and no gel in electron irradiation up to high doses. The second evidence was the change of glass transition temperature(Tg); Tg did not decrease with dose in ion irradiation and decreased much in electron irradiation. These evidences mean that both of PES and U-PS undergo crosslinking by ion irradiation and chain scission by electron irradiation. The difference of mechanical properties in Fig.2 is caused by the chemical reaction as crosslinking and chain scission.

For aliphatic polymers which is crosslinking or chain scission type by irradiation, there is no difference on the irradiation effects between ion and electron. However, for aromatic polymers the chemical reactions are different to result the difference in the mechanical property. The reason of the difference would be expected to explain by the LET. But, it seems to have difficulty why only aromatic polymer is affected by LET.

At present, it is thought that there are two factors in the ion irradiation effects of polymer materials. The one is the LET effect, that is, the chemical reaction in polymer matrix with high LET proceeds mainly in the local area as inside of ion track, because the reactive species would be much high concentration in the local area and the reaction mechanisms are different from the low LET. The other factor is the thermal effects during irradiation, which means the heating of bulk polymer by high dose rate in case of ion. The irradiation effects of polymers are affected by the irradiation temperature, and the effect depends on the polymers. For PES, it was observed that the chemical reactions is changed by temperature of polymer during irradiation in case of gamma-rays and electrons irradiation, that is, the chain scission is predominant at lower temperature and crosslinking increases at higher temperature. In our ion irradiation, beam scanning technique was applied to prevent the increase of specimen's temperature. However, the temperature of specimen in the area of beam spot might be increased because the scanning rate of perpendicular is rather small.

In order to clear the LET effect, the temperature dependency on the effect during irradiation must be evaluated.

References

(1) W.G.Burns and J.R.Parry, Nature 201, 814(1964).
(2) A.Licciardello, O.Puglisi, L.Calcagno and G.Foti, Nucl.Instrum.Meth.Phys. Res.(B), 32, 131(1988).
(3) T.Sasuga, S.Kawanishi, T.Seguchi and I.Kohno, Polymer, 30, 2054(1989).
(4) T.Sasuga, H.Kudoh and T.Seguchi, JAERI TIARA Annual Report, 177(1992).
(5) H.A.Bethe and J.Ashkin, "Experimental Nuclear Physic", Wiley, New York, (1953).
(6) S.M.Selzer and M.J.Berger, J.Radat.Phys.Chem., 33, 1189(1982).

Table 1. Stopping Power of Ions in Polymers

Polymer	Stopping Power(MeV cm^2/g)		
	H^+ / 10MeV	He^{2+} / 50MeV	e^- / 2MeV
Polyethylene(PE)	44.0	142	1.77
Polytetrafluoroethylene(PTFE)	27.4	121	1.72
Polyethersulphone(PES)	40.7	131	1.78
Cellulose tri-acetate(CTA)	41.0	138	1.77

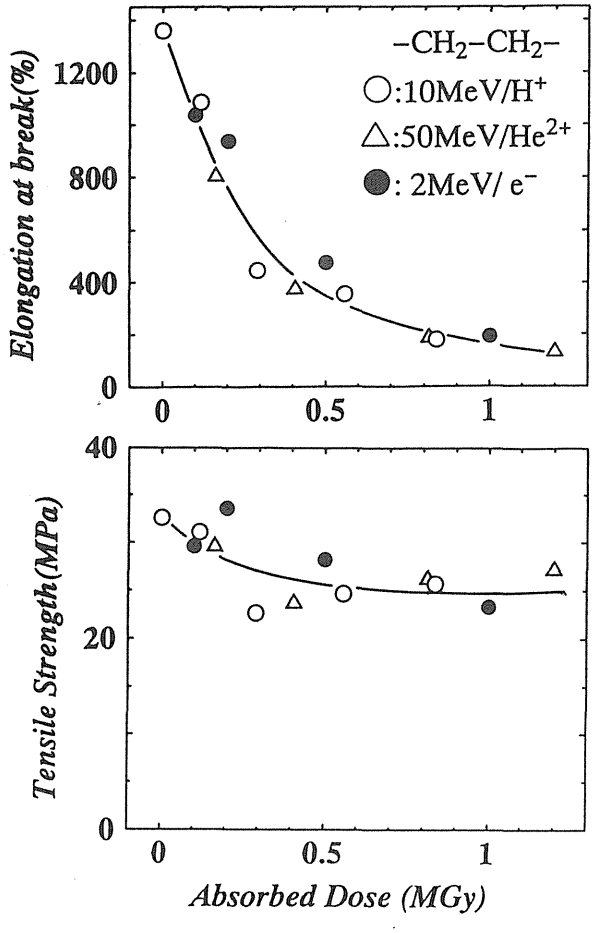

Fig.1 Changes of Mechanical Properties of Polyethylene Film irradiated by ions (H^+, He^{2+}) and electron.

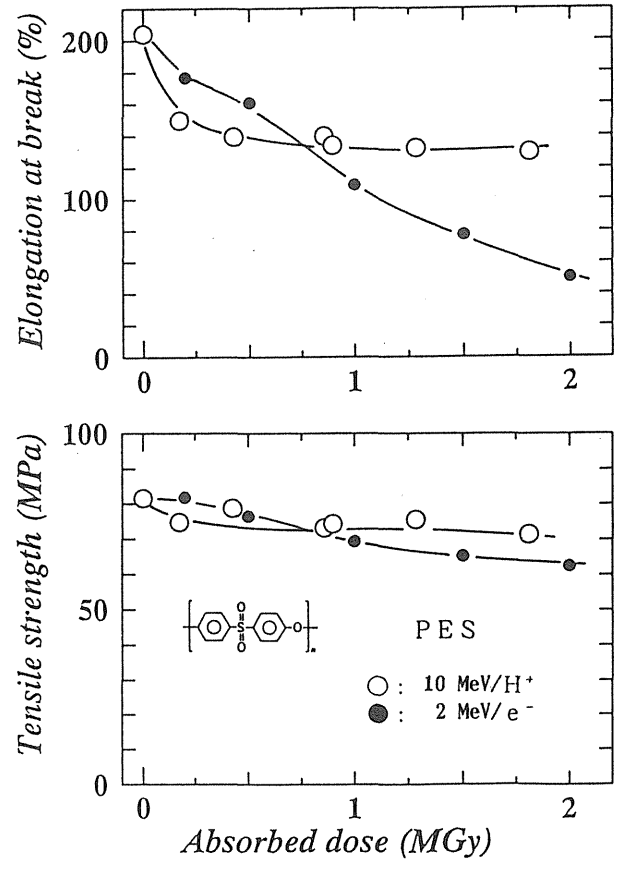

Fig.2 Changes of Mechanical Properties of Polyethersulphone film irradiated by H^+ and electron.

MICRO PROFILE OF THE CHEMICAL STRUCTURE IN ION-BEAM IRRADIATION EFFECTS FOR SOME POLYOLEFINS.

Yoshimasa Hama, Atsuki Katou, Kenichi Hamanaka, Hideya Matsumoto
Advanced Research Center for Science and Engineering, Waseda University, 3-4-1 Okubo, Shinjuku-ku, Tokyo 169, Japan
Hisaaki Kudou, Tsuneo Sasuga, Tadao Seguchi
Japan Atomic Energy Research Institute, Takasaki Radiation Chemistry Research Establishment, 1233 Watanuki-machi, Takasaki 370-12, Japan
Fumio Yatagai
The Institute of Physical and Chemical Research (RIKEN)
Hirosawa 2-1, Wako-shi, Saitama 351-01, Japan.

Abstract.

The depth profile of the change of the chemical structure in some polyolefins such as polyethylene, polypropylene induced by ion-beam irradiation is investigated with micro-FT-IR method. The predominant species produced by ion-beam irradiation were the double bond, carbonyl group and hydroxyl group. The damage in polypropylene by irradiation was rather smaller than in polyethylene. The depth profile of these species is similar to the Bragg curve. The G-values for production of these species were calculated. It is found that the dose dependence of the G-value decrease with increase of absorbed dose. The carbonyl groups are produced in vicinity of the surface of the polymer sheet in the case of low absorbed dose.

Introduction.

It has been reported that one of the important process of the degradation of polymers irradiated by γ -rays or electron beam is the oxidation reaction between radicals induced by irradiation and oxygen molecules diffusing into the polymer. If a slab of polymer is irradiated in air, the oxidation reaction would be induced much more in the surface region than in the inner region. Because, most of oxygen molecules diffusing into the polymer react with radicals in vicinity of the surface to be consumed, so that radicals left in the inner region react almost to go to recombine each other. The probability of these reactions should be dependent of the

irradiation condition such as a dose rate, temperature a atmosphere pressure, a rate of reaction, a diffusion constant of oxygen molecule and so on.

On ion-beam irradiation, different effects would be expected because of the high LET. The depth profile of the stopping power would be expected to give different profile of the concentration of radicals produced along the track. This results in making different distribution of the change of the chemical structures in the polymer. This is very important to estimate the degradation of polymer irradiated by ion-beams.

This report concerns the depth profile of the chemical structure change in some polymers induced by ion-beam irradiation and the irradiation condition dependence of the chemical reaction.

Experimental.

In this work, low density polyethylene (LDPE), high density polyethylene (HDPE) and polypropylene (PP), which were formed in a slab of 2mm thick, were used.

H^+ and He^{2+} were irradiated in vacuum with AVF cyclotron in JAERI Takasaki (TIARA). C^{6+} was irradiated in air with Ring cyclotron in Riken. The absorbed dose at the surface was estimated by beam current.

The sample irradiated was sliced along the cross-section to the slab surface and a thin film of about 100 μm was obtained.

The infrared spectrum data from the region of 30μm x 30μm of the thin film were accumulated stepwisely along the depth direction by using micro-FT-IR spectrometer (JEOL JIR micro-6000).

Results and discussion.

Depth profile of the structure change induced by irradiation.

When LDPE or HDPE was irradiated in vacuum by ion-beam (10MeV H^+, 20MeV H^+ or 20MeV He^{2+}) and then measurement was carried out in air, predominant chemical species induced were trans-double bond($\sim$640cm^{-1}), carbonyl group($\sim$1720cm^{-1}) and hydroxyl group($\sim$3200cm^{-1}). The depth profiles of these species are similar to Bragg curve as shown in Figs.1 and 2 . The fact that the carbonyl groups could be observed and the profile was similar to Bragg curve, nevertheless irradiation was carried out in vacuum, indicates that production of carbonyl groups comes from the reaction of allyl radicals with oxygen molecule which is

occurred after the irradiated sample is exposured to air. The allyl radical produced in PE is stable in vacuum at room temperature. This is supported by the fact that double bond formation only was observable for PP in which there are no stable radical at room temperature which can react with oxygen molecule to produce carbonyl group.

When PE was irradiated to a dose of 17.5kGy in air by 135MeV/n C^{6+}, very thin layer on the surface was oxidized (Fig.3). On the other hand, in inner region the trans-double bond was produced and the depth profile is the same as in the case of proton irradiation in vacuum.

G-values for species and their dose dependence.

G-values for the trans-double bond and carbonyl group were calculated by using the stopping power and the IR absorption intensity for each sample. A depth profile of the G-value for trans-double bond obtained for LDPE irradiated by H^+ is shown in Fig.4. All other results also are similar to that of LDPE. It can be found that the G-value decreases with the depth, that is, with increase of the stopping power. This is coincident with the results of the irradiation time dependence (in other words, absorbed dose dependence) of the G-value at every depth. This suggests that the species produced precedingly are destroyed to change another species by successive irradiation.

On the other hand, the G-value for trans-double bond for LDPE irradiated by 20MeV H^+ was found to be larger than that for LDPE irradiated by 20MeV He^{2+}. This is attributed to difference of their stopping power.

Irradiation effect of PP.

The ion-beam irradiation effects of PP were found to be little compared with those of PE on FT-IR measurement. In PP, double bond formation is predominant on irradiation in vacuum. On irradiation to dose of 17.5kGy by C^{6+} in air, the change of chemical structure was hardly observed.

Conclusion.

The irradiation effects of ion-beams for PE and PP are different from that of γ -rays or electron-beams. Most of the depth profile of the change of chemical structure by ion-beam-irradiation are similar to Bragg curve, corresponding to the energy profile. It is very convenient that various chemical changes corresponding to the energy profile of ion-beam could be observed together on every spectrum by using the micro-FT-IR measurement.

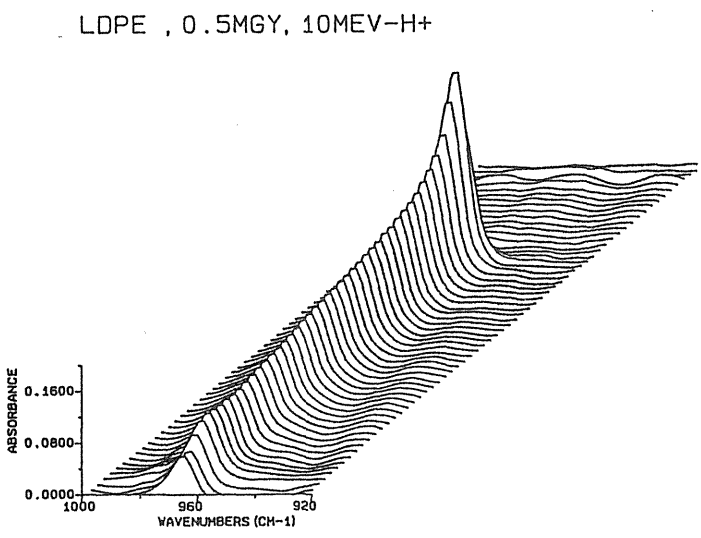

Fig.1. Depth profile of the absorption due to trans-double bond observed for LDPE irradiated to a dose of 0.5 MGy by 10MeV H^+.

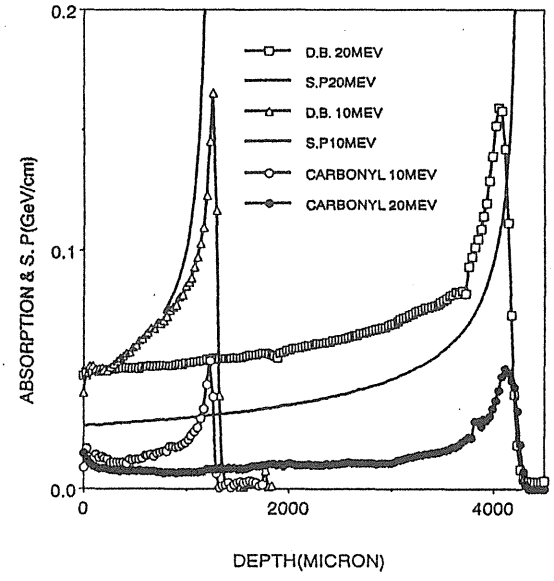

Fig.2. Depth profile of the trans-double bond (D.B) and carbonyl group obtained for LDPE irradiated to a dose of 0.5 MGy by 10MeV or 20MeV H^+. The stopping power (S.P.) curves calculated are shown in solid lines.

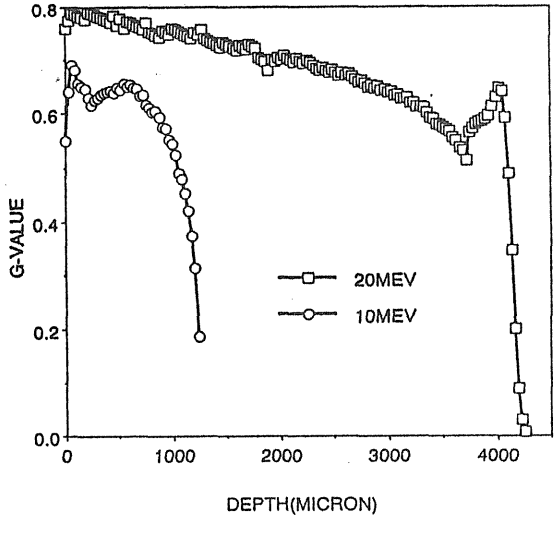

Fig.3. Depth profile of G-value for trans-double bond obtained for LDPE irradiated to a dose of 0.5 MGy by 10MeV or 20MeV H^+.

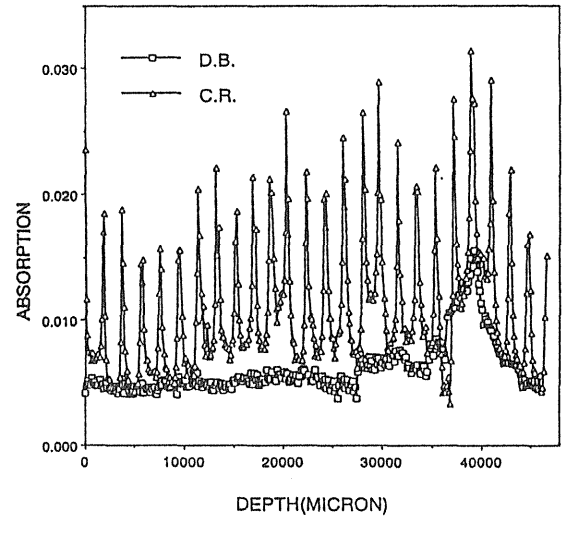

Fig.4. Depth profile of the trans-double bond (D.B.) and the carbonyl group (C.R.) obtained for HDPE irradiated in air to a dose of 17.5 MGy by 135MeV/n C^{6+}.

HIMAC COMMISSIONING STATUS

T. MURAKAMI
Division of Accelerator Physics and Engineering
National Institute of Radiological Sciences
4-9-1 Anagawa, Inage-ku, Chiba 263

Abstract : The heavy-ion synchrotron of HIMAC began commissioning in November, 1993, and succeeded in accelerating and extracting ^{4}He beams of 230 MeV/u, while the injector linac has been successfully operated from April, 1993. For the efficient use of the accelerator, three clinical-treatment rooms and four experimental rooms for basic science have been prepared.

I. Introduction

A heavy-ion synchrotron facility, HIMAC (Heavy Ion Medical Accelerator in Chiba) at NIRS (National Institute of Radiological Sciences), is nearing completion. HIMAC was designed and constructed for medical use, especially for cancer treatment, as one of the big projects of the "Comprehensive 10 year Strategy for Cancer Control". It can accelerate beams from ^{4}He to ^{40}Ar to 600 MeV/u, corresponding to a maximum range of 30 cm in tissue, with a high dose rate of 5 Gy/min. The first clinical treatment will start in early 1994, following the biological-data compilation required for treatment.

Because Bevatron at LBL closed down, no other accelerators exist which can deliver heavy-ion beams within this energy range, except for SIS at GSI in Germany. Therefore, not only clinical use, but also applications to a variety of fields utilizing heavy-ion beams, including biology, physics, and chemistry, are strongly desired for the efficient use of HIMAC. The versatility of the two-ring structure combined with 24-hour operation can realize the delivery of beams for clinical treatments and experiments without any interference. In order to utilize these beams, three clinical-treatment rooms and four experimental rooms for basic science have been prepared.

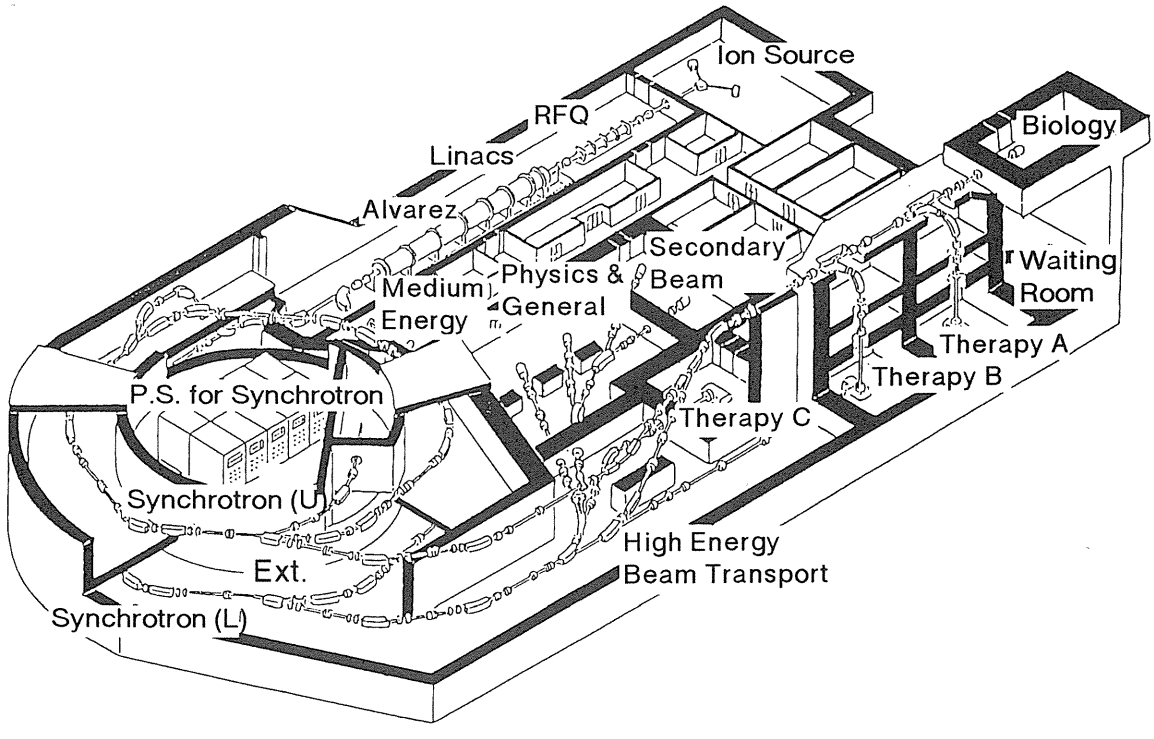

Fig. 1. Bird's-eye view of the HIMAC facility.

II. Design and Status of the Accelerator

Figure 1 shows a bird's-eye view of the HIMAC facility. It comprises ion sources, an injector, a synchrotron with two rings, a beam-transport system, three treatment rooms, and four experimental rooms. The specifications and parameters of the accelerator are summarized in Table 1 (the injector) and Table 2 (the synchrotron). Readers can refer to the HIMAC report[1] for details concerning the accelerator design.

Table 1. Injector specifications.

Ion species	$^{4}He - ^{40}Ar$
Charge to mass ratio (q/A)	$\geq 1/7$
Ion source type	PIG & ECR
Frequency	100 MHz
Repetition rate	3 Hz Max.
Duty factor	0.3% Max.
RFQ linac	
Input / Output energy	8 / 800 keV/u
Vane length	7.3m
Cavity diameter	0.59m
Peak rf power	260 kW (70% Q)
Alvarez linac	
Input / Output energy	0.8 / 6.0 MeV/u
Total length	24m (3 rf cavities)
Cavity diameter	2.20 / 2.18 / 2.16 m
Peak rf power	840 / 830 / 770 kW (75% Q)
Output beam emittance	$\leq 1.5\pi$ mm-mrad (normalized)
Momentum spread	$\leq \pm 1 \times 10^{-3}$

Table 2. Synchrotron specifications.

Maximum rigidity	9.75 Tm
Dipole field at full rigidity	1.5 T
Quadrupole gradient at full rigidity	7.4 T/m
Lattice type	FODO
Circumference	129.6 m
Super-Periodicity	6
Cells per period	2
Long / Short straight section length	5.0 / 0.8 m
Injection energy	6 MeV/u
Output energy (^{4}He - ^{28}Si, q/A=1/2)	100 - 800 MeV/u
(^{40}Ar, q/A<1/2)	100 - 600 MeV/u
Maximum intensities for light ions	10^{11} ppp
Repetition rate	0.3 - 1.5 Hz
Extraction	Slow extraction
Vacuum	5×10^{-9} Torr
Betatron tunes Q_H / Q_V	3.75 / 3.25

Two types of ion sources, PIG and ECR, were prepared to produce a variety of ion beams. The injector comprises two types of linacs, RFQ and Alvarez, and accelerates the beams up to 6

MeV/u. Most of the ion species are charge-stripped to a charge-to-mass ratio of 1/2 by a carbon-foil stripper installed at the exit of the Alvarez linac. The synchrotron has two identical rings (upper and lower) and accelerates beams in the two rings alternatively by pulse-to-pulse operation. The two-ring structure maximizes the efficiency of the facility, since the beams can be delivered into two courses simultaneously.

Both of the ion sources have shown satisfactory results, supplying beams with sufficient intensity and stability. The injector linac started accelerating beams in April, 1993;[2] since then it has successfully accelerated beams of ^{4}He, ^{12}C, ^{16}O, ^{20}Ne, and ^{40}Ar. The beam characteristics exceed the specifications. The development of ion sources is also being carried out in order to produce heavier ions, such a Fe or Kr. The synchrotron began commissioning in November, 1993, and succeeded in accelerating ^{4}He beams of 230 MeV/u within a month. Beams with a spill length of ~400 ms were extracted and transported to all of the beam courses. An effort to increase the acceleration and extraction efficiencies is being continued. The ^{4}He beam is requested to evaluate the accelerator performance and to confirm the shielding capacity of the building, while the clinical treatments will be carried out using ^{12}C beams of 290 MeV/u.

III. Treatment Rooms and Experimental Rooms

There are three clinical treatment rooms (rooms A, B, and C), equipped with horizontal courses (rooms B and C) and/or vertical courses (rooms A and B). Each course has a wobbling system which accomplishes a uniform irradiation field within ±2% with a size of 22cm ϕ. A ridge filter is used to spread the narrow Bragg peak to the broader one and a range shifter precisely controls the beam energy.

Four experimental rooms for basic research have been prepared: 1) a biology room (BIO), 2) a general-purpose and physics room (PHY), 3) a secondary-beam room (RIB), and 4) a medium-energy beam room (MEXP).

The same wobbling system as that used in the treatment room was also installed in BIO in order to offer a beam with the same characteristics. In BIO, irradiation experiments on cells or small-size animals will be carried out. PHY is fortified by heavy radiation shields so that one can handle beams having maximum energy and intensity. PHY has two beam courses and much space around them. RIB is a room placed next to PHY for the construction of a secondary beam course in the future. The spill length of the synchrotron beam is now around 400 ms using a slow-extraction system.

In MEXP, 6 MeV/u beams from the injector are available. The spill length can be varied between 20 and 500 μs and the maximum beam intensity is around 800 μA for ^{4}He. Since the switching magnet which bends the beam to the MEXP course operates in a pulsed mode, the injector can deliver beams to both the synchrotron and MEXP alternatively. The beams are, therefore, delivered to the two synchrotron rings and the MEXP course in a pulse-to-pulse mode. The entire system works very satisfactorily in this operational mode. The acceleration of different ion species from pulse to pulse (time-sharing acceleration) is under consideration to enhance the versatility of HIMAC.

From late 1993, the preparation of a few trial experiments began in MEXP. Included are "Microscopic ion-beam pulse radiolysis", "Search for isomeric states by gamma-ray spectroscopy", and "Secondary electron emission from water by heavy-ion impacts".

References

1) Y. Hirao, et al., NIRS-M-89, HIMAC-001 (1992) 1.
2) T. Murakami, et al., Proc. 1993 Particle Accelerator Conference, to be published.

LINEAR ENERGY TRANSFER DEPENDENCE OF FREE RADICAL FORMATION IN ION-IRRADIATED ALANINE

HITOSHI KOIZUMI, TSUNEKI ICHIKAWA AND HIROSHI YOSHIDA
Faculty of engineering,
Hokkaido University
Kita-ku, Sapporo 060,
Japan

Abstract

Radical formation in alanine dosimeter irradiated with ion beams has been investigated. Dependence of G-value of the radicals on the ion beams and irradiated fluence has been examined. Average radius of radical distribution along ion tracks has been estimated from relationship between the radical yield and fluence. The radius is about 4-6nm for 0.5MeV-3MeV H^+ and He^+ beams, while the radius is 20-30nm for 175 MeV Ar^{8+} and 460 MeV Ar^{13+} beams.

Introduction

Radiation effects of ion beams much depend on energy and species of the ions. It is attributed mainly to the difference of local distribution of deposited energy in materials. Local distribution of reactive intermediate are then important to elucidate mechanism of chemical reactions induced by ion beams. In this paper, we report the results of study on the radical formation in ion beam-irradiated alanine[1]. In alanine crystal, radicals are produced with very high efficiency, G=7.6[1, 2] and they are very stable even at room temperature. It means the produced radicals little migrate in the crystal. The local distribution of the resulting radicals will then reflect their initial distribution, and it is convenient to elucidate the relation between the local distribution of the dose and that of the radicals.

Experimental

The alanine film dosimeter supplied by Takasaki Research Establishment, Japan Atomic Energy Research Institute(JAERI) were used as a sample[3].They are made of alanine powder and low-density polyethylene as binder. The film of 160μm thickness with the 50:50wt% ratio of alanine/LDPE and the one of 220μm

thickness with the 60:40wt% ratio of alanine/LDPE were used. 0.5 MeV-3MeV H^+ and He^+ ions were irradiated with the Van de Graaf accelerator at H.I.T., University of Tokyo.The samples were irradiated one side homogeneously with swept ion beam through a window of 7mm diameter in vacuum at ambient temperature. 175MeV Ar^{8+} and 460 MeV Ar^{13+} were irradiated with the cyclotron accelerator at TIARA, Takasaki Research Establishment,JAERI. The dose distribution at the sample were measured with RCD and Guf film dosimeters and the radius of the beam at the sample was 6-6.5mm^2.

The free radicals were measured with X-band ESR spectrometers at Hokkaido University and JAERI.Their yield was determined with DPPH as a reference.

Results and Discussions

Figure 1 shows the radical yields in the H^+ and He^+ irradiated samples as a function of ion fluence. The ion fluence is the number of irradiated ions per unit area.Lower than the critical fluence the yields is constant, while higher than it the yields much decrease. Although the linear energy transfer(LET) and velocity are different one another, the critical fluences are nearly the same among the ion beams: that is about 10^{12}ions cm^{-2}. The decrease of the yield in the higher fluence is due to the overlap of ion tracks, and the reciprocal

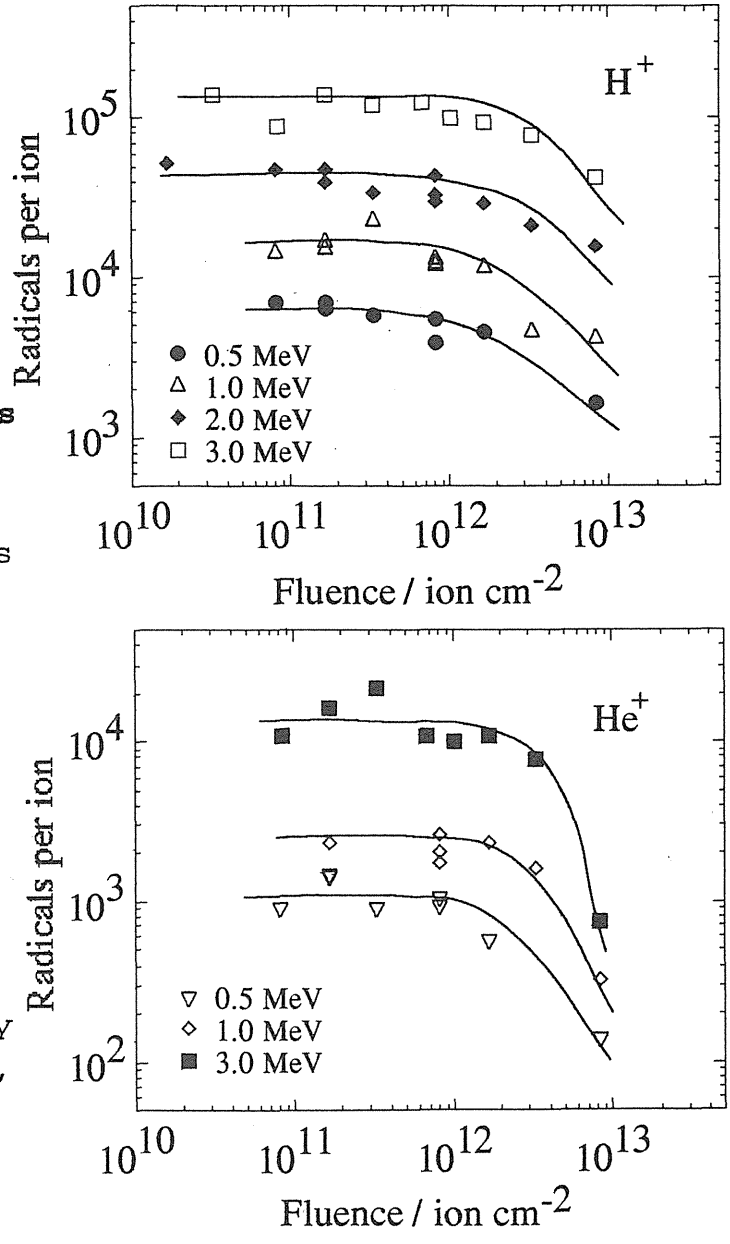

Fig.1.Radical yield in alanine dosimeter as a function of ion-fluence produced by irradiation of 0.5 MeV-3 MeV H^+(upper) and He^+ ions.

of the the critical fluence gives the average cross section of the ion tracks. The radius of the ion tracks are then 4-6nm for 0.5MeV-3MeV H^+ and He^+ ions. The results for 175MeV Ar^{8+} and 460MeV Ar^{13+} are shown in figure 2. The yields are also nearly constant lower than a critical fluence, and they much decrease higher than the fluence. The critical fluence, however, is much lower than that for H^+ and He^+ ions: that is about 5 X 10^{10} ions cm^{-2}. This critical fluence gives the average radius of the ion tracks as 25nm.

To elucidate the relation between the local distribution of the radicals and of the deposited energy, we have calculated the radial dose distributions of an ion track. An equation proposed by Chatterjee et al.[4] was used. In their equation ion track are divided to two region, namely core and penumbla. The core is a region where energy is deposited with high density along an ion trajectory. The penumbla is a region surrounding the core, where energy is deposited by recoil electrons. Relative shape of the radial distribution is only a function of the velocity of the ion. Both the radius of the core and that of the penumbla increase with increasing the ion velocity.If the radicals are produced in response to the

Table 1. Radius at the dose of 10^5 Gy ($r(10^5Gy)$)

Ion	Energy / MeV	$r(10^5Gy)$ / nm
H	0.5	1.0
	1.0	0.75
	2.0	0.57
	3.0	0.69
He	0.5	2.8
	1.0	2.7
	2.0	2.0
	3.0	1.7
Ar	10	8.5
	25	8.4
	50	7.8
	100	6.9
	175	6.0
	460	4.4

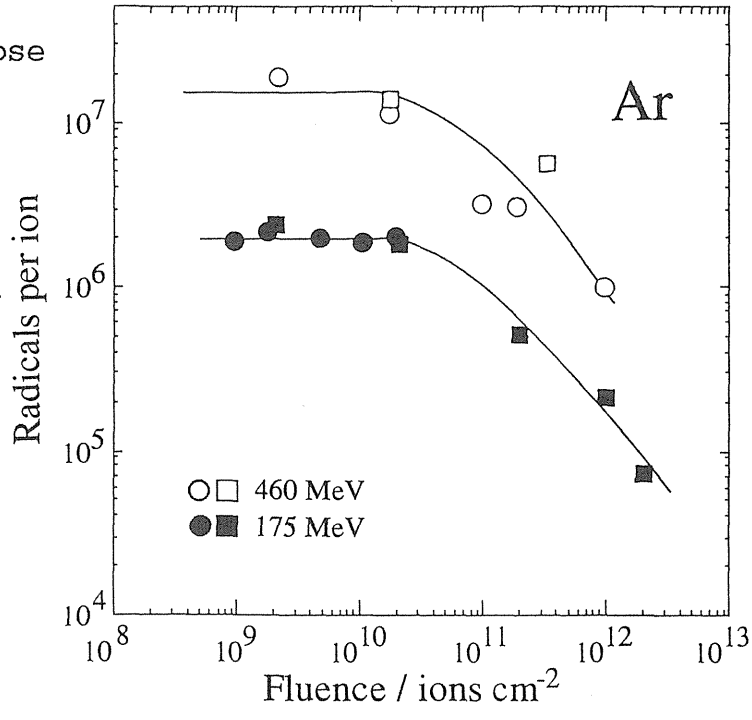

Fig.2 Radical yield in alanine dosimeter as a function of ion-fulence produced by irradiation of 175 MeV and 460 MeV Ar ions.

initial local dose distribution in the track, the radius at the dose of 10^5 Gy gives the radius of the radical distribution. Since the G-value of gamma-irradiated alanine starts to decrease at the critical dose of 10^5 Gy, overlap of the region of the dose higher than 10^5 Gy cause decrease of the radicals. The radii at the dose of 10^5 Gy are shown in table 1. They depend on the ions, and they are smaller than the radii of the radical distribution. This indicates that the distribution of radicals spreads from the local dose distribution.The radius of the radical distribution is mainly determined by the diffusion of the radiation energy in the track.Positive charges are generated densely in core by ion beams. Coulombic repulsion between the cations pushes them outward to expand the core. They migrate and recombine with electrons to generate the free radicals. The obtained radii indicate the precursors of the radicals migrate about several nm in the H^+ and He^+ irradiated samples, while they migrate 10-20nm in the Ar irradiated ones.

This work has been carried out in collaboration with Hiromi Shibata, Yoichi Yoshida, Seiichi Tagawa of University of Tokyo, and Hideki Namba, Takuji Kojima, Mitsumasa Taguchi of Japan Atomic Energy Research Institute.

References

1. V. V. Krushev, H. Koizumi, T. Ichikawa, H. Yoshida, H. Shibata, S. Tagawa and Y. Yoshida. *Radiat. Phys. Chem.* (1994) in press.
2. T. Henriksen, T. Sunner and A. Pihi. *Radiat. Res.* **18**, 147 (1963).
3. T. Kojima, H. L. A. Ranjith, Y. Haruyama, S. Kashiwazaki and R. Tanaka. *Appl. Radiat. Isot.* **43**, 41 (1993).
4. J. L. Magee and A. Chatterjee. in *Kinetics of nonhomogeneous processes* , edited by G. R. Freeman (John Wiley & Sons, New York, 1987) chap.4.

Track-Depth and Time Resolved Dynamics of Excited States in Ion Tracks: Effects of High-Decnsity Excitation

Kazuie Kimura
RIKEN, Wako Saitama 351, Japan

Abstract

A track scope developed enables to make the first observation of differential intensities dL/dx and efficiencies dL/dE of condensed helium along the N-tracks. Luminescences are assigned to Rydberg states of excimers produced by the bimolecular reaction of the lowest triplet excimer, ^3a. Increasing ion penetration enhances this reaction, but near the track termination, reactions of three ^3a dissociates ^3a. There appears an additional peak of dL/dE. Ion irradiated BaF_2 reveals Auger-electron free luminescence whose decay is guite different from SR-light irradiation. The mechnisms is explained.

One of the most important radiation effects of heavy-ion irradiation in condensed matter is the high-density excitation of electrons in an outermost shell.[1] Energy deposition can amount to as much as 1000 V per Angstrom near the termination of the ion track. Morever, additional effects such as charge-exchange and direct excitation become important there. Other radiation effects characteristic in solids are also important in this region. What changes are actually caused in matter by such radiation effects and how the depth dependence along the ionic track is, are important unsolved problems. Then, we have developed a track-scope and a fast measurement technique of luminescence decay. At present, these apparates can give data with the highest resolution in space and time.

The track scope was composed of a 1 m imaging fiber-bundle of 10000 quartz fibers with a square cross section of 2 x 2 mm and a position-sensitive photon counter(SMA).[2] Since the track length of few MeV ions is too short in usual liquid and solid targets (less than a tens μ m) to be resolved, the track length was extended using the vapour or cluster of samples. In this review, the sample was helium whose cluster could be obtained easily.

Measurements of fast luminescence decay was made by single-ion hitting and single-photon counting techniques (SISP) developed.[3]

Origines of luminescences from N-ion irradiated helium

As known in studies by means of discharge and electron-irradiation, observed luminescences at lower helium presure than few Torr originate from a number of excited helium atoms. With increasing pressure, principal radiative excited states turn to excited diatomic helium ie. excimers. Intensity of excimer luminescence exhibitted a drastic change with a sharp peak at about 0.01 g/cm^3. The rising part towards the peak was explained in enhanced regeneration reactions.[4,5]

$$^3a + {}^3a \longrightarrow {}^3d,\ {}^1D,\ {}^1J,\ {}^1H,\ \text{and}\ {}^1A \qquad (1)$$

The descending part was explained in the instabilization of Rydberg states by reducing radius of the bubble (cavity) or its instability with increasing density.[6] The Rydberg state of the excimer has the large orbital radius and is stabilized in the bubble. Thus, increasing density decreases luminescence intensities and number of their peaks in order of the radius of the excimer. At the density larger than 0.03 g/cm^3 interested in this review, only four peaks due to ^{3}d-^{3}b, ^{1}D-^{1}B, ^{1}J-^{1}C, and ^{1}H-^{1}C , were observed (Fig. 1).

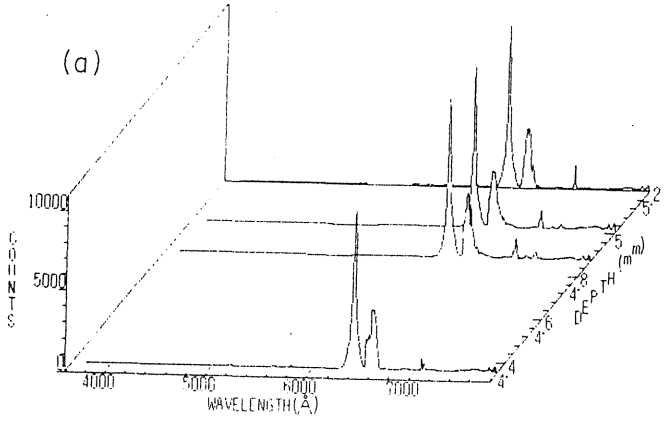

Fig. 1. Track-depth dependent luminescence spectra of N-ion irradiated helium at the density of 0.02552 g/cm^3, illstrated in equal maximum height. Peaks except for ^{3}d - ^{3}b are 10 times enlarged.

No further eliminations of peaks occurred even in liquid phase. It is concluded that these excimers are formed by the same formation reaction, ie. Eq. 1, from the result that relative intensity ratio among the four peaks were scarcely invariant to the variation of both the density and the depth of track, as shown in Fig. 1.[6].

Excimer dynamics along the ion track

Figure 2 shows dL/dx along ion track at various helium densities. Next, let analyse Fig. 2 with conversion of track length into several variables such as stopping power, range, excitation density, ion energy, and ion velocity. Each dL/dx curve in Fig. 2 has a peak maximum and the peak shifts with increasing density. These shifts

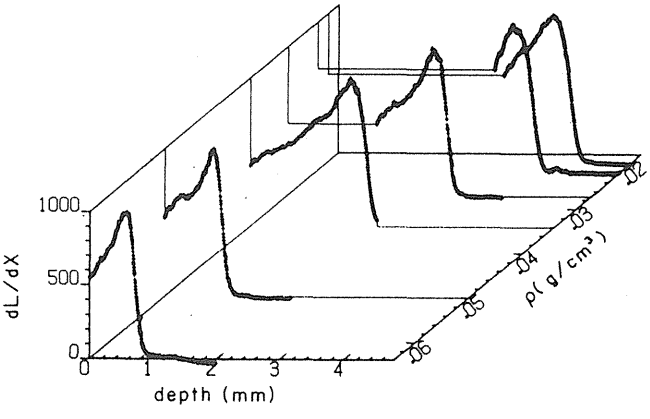

Fig. 2. Differential luminescence of UV and VIS light, dL/dx, vs. the depth of N-ion track, illustrated in equal maximum heights.

appeared also on the plots using the range, stopping power and ionic energy instead of the depth. However, the peaks converged at the same position, when dL/dx was plotted as a function of energy deposition per unit volume (the excitation density).[2,5,6] In conclusion, the increase in dL/dx with increasing excitation-density (namely, with deeper propagation of ions) originates from enhanced reaction (1) because of dense ^{3}a. With further increasing excitation

density, dL/dx attains a peak and then decreases rapidly near the track termination. This can be explained by the following new reaction. Namely, the extremely high concentration of ^3a leads to nonradiative reaction:

$$^3a + {}^3a + {}^3a \longrightarrow \text{dissociative} \quad (2)$$

An additional Bragg peak in luminescence efficiency dL/dE

The dL/dE vs. excitation density reveals the additional peak marked by the arrows at deep penetration(Fig. 3).

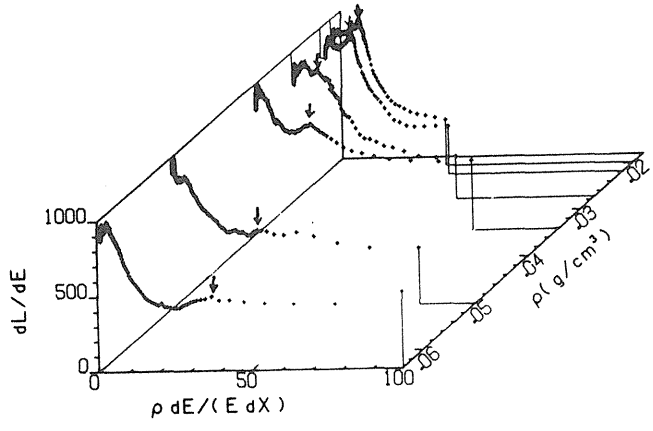

Fig. 3. dL/dE vs. excitation density by N-ion irrqadiation. Arrows show the second peaks.

The peak may be called the additional Bragg peak. The peak shifts with the helium density, but they coincided at about 4 x 10^8 cm/s by plotting dL/dE with the ionic velocity. The additional peak suggests additional excitation processes. Charge exchange and direct excitations were proposed as such processes.[2,5,6] It is important and interesting whether the additional peak can be obeserved generally.

As shown briefly, our track-depth resolved measurement can inform many important new excited states and reactions and their dynamics all of which compose ion irradiation effect. Further studies on other rare gasses, water, and solid are in progress.

Auger-electron-free luminescence of core exciton and excitation-density dependence

The decay time of Auger-electron free luminescence of ion irradiated BaF_2 was found to decrease with increasing excitation density.[3] The decay was approximated to the exponential at the initial and final stages, in contrast with a single exponential for SR-light irradiation. The fast decay time decreased with increasing excitation density, while the slow one was invarient (Fig. 4a).

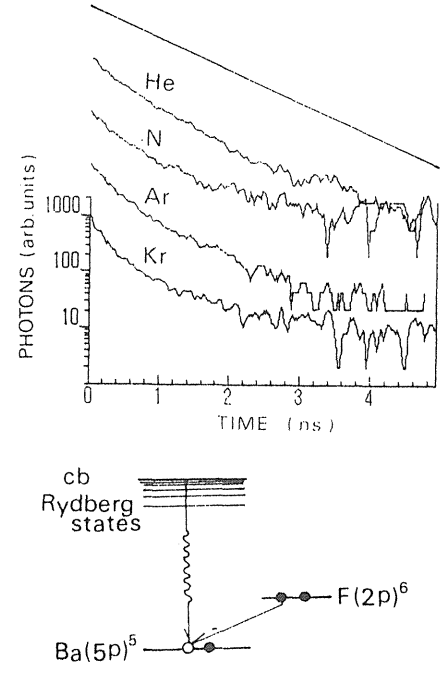

Fig. 4. a): decay of Auger-electron-free luminescence for 1.5 MeV/amu ion-irradiated and photoirradiated BaF_2. b): A competition between nonradiative recombination and Auger-electron-free luminescnece.

A model with decreasing Auger-electron free transitions (from 2p of F atom to 5p core hole of Ba atom) which compete with nonradiative recombinations between core holes and quasi-free electrons could explain the result.(Fig. 4b) Kinetics enabled to estimate the lifetime of the outermost core exiton due to Auger-electron-free luminescence.

References

[1] K. Kimura, T. Matsuyama, and H. Kumagai, Radiat. Phys. and Chem. 34, 575(1989).
[2] K. Kimura, Nucl. Instr. and Meth. B53, 301(1991).
[3] K. Kimura and J. Wada, Phys. Rev. B48, (1991) in press.
[4] K. Kimura, J. Chem. Phys. 84, 2002(1986); ibid. 84, 2010-(1986). [5] K. Kimura, Nucl. Instr. and Meth. A327, 34(19-93).
[6] K. Kimura, Phys. Rev. A47, 327(1993)

SPECIAL LECTURE: WHAT A RADIOBIOLOGIST EXPECTS FROM RADIATION CHEMISTRY?

S. OKADA
Nuclear Systems Association
2-13-6 Shimbashi, Minatoku,
Tokyo, Japan

Abstract

Elucidation of primary mechanisms of 'important' radiobiological phenomenon (cell death, mutation, carcinogenesis etc.) at molecular level is a challenge to radiation chemists. To do so, radiation chemists have to learn to handle living biological systems through a few years of apprenticeship. This will not only open new area in radiation chemistry, but also in radiobiology.

Ionizing radiation will induce various types of damages on cellular molecules, proteins, carbohydrates, lipids, DNA and RNA etc.. Among them, the hereditary information carrier DNA, would be likely to be the target of important radiological phenomenon (e.g., cell killing, mutations, carcinogenesis etc.). Radiation damages on DNA include single-strand scissions, double-strand breaks, base damages, sugar damages, scission of glycosyl bonds, uncoiling of chromatin supercoils, etc.. Most of DNA damages would be restored by various cellular repair enzyme systems. Only a very few would be non-repaired or mis-repaired or mis-replicated, resulting in chromosome aberrations, cell killing, mutagenesis and carcinogenesis.

Let's take one example of high LET radiations: When mammalian cells were irradiated by neutrons, RBE of 2 was obtained for cell killing. Three types of DNA scissions, single-strand breaks, double strand breaks and non-reparable breaks were observed to have RBE of 0.3, 1 and 1.3, respectively. Non-reparable breaks

gave a dose response curve of a linear quadratic type with the highest RBE, similar to that of cell killing. Other evidences, modification of radiosensitivity with radical scavengers, with oxygen, cell-cycle dependency, sublethal damage repair, etc., also showed parallel relationship between non-reparable breaks and cell killing. Here, what we like to ask radiation chemists are mechanisms of primary events of radiobiological phenomenon on DNA molecules in living cells. For example, how double strand breaks and of non-reparable breaks of DNA are produced in living cells. Especially, what is the nature of multiple damaged sites. A spectrum of all types of radiation damages on DNA in living cells are another problem we like to know.

In radiobiology, problems of radiation oncology (diagnosis, , therapy, beam control, biological basis) have been challenges to all the disciplines of radiations. Radiobiology at low doses (1-100 mSv) and low dose rate (down to 1 mSv per year) for quantitating radiation risk, are becoming new area to be explored. Molecular epidemiology, also for risk evaluation, will be another new area. One of the future area will be 'radiation chemistry of the gene (e.g. p53)', which could be the basis of molecular epidemiology. In high IET radiation field, track structure and its radiobiology, types of heavy ions which show effective cell killing with less efficient mutations (carcinogenesis), space radiobiology are some of the problems.

Radiobiology will welcome radiation chemists to explore these problems with their knowledges of radiation chemistry and with introduction of new refined methodology.

References

1. K. Sakai, S. Suzuki, N. Nakamura and S. Okada; Induction and subsequent repair of DNA damage by fast neutrons in cultured mammalian cells. Radiat. Res. 110, 311-320 (1987).

2. S. Okada; Molecular mechanisms of radiation-induced cell killing. Taisha (Metabolism) 21(10), 1155-1168, 1984.

An Experiment on Primary Chemical Processes by Using High Energy Heavy Ion from HIMAC

Y. Yoshida

The Institute of Scientific and Industrial Research, Osaka University

8-1 Mihogaoka, Ibaraki, Osaka 567, Japan

An important chemical effect of high energy heavy ions is the production of ionized species, such as electrons and radical cations, because the chemical processes starts from these species. Particularly, the initial spatial distribution of these species produced by the ion beams, so-called high LET radiation, is very different from those by the electron and g-ray, because of the high-densed excitation. Therefore, the primary processes of heavy ion beams must be different

New studies on the primary processes induced by high energy heavy ion have been started in HIMAC. The elucidation of the following points are expected.

a) Effects of the high-densed excitation in the primary processes.

b) Effects of the structure of track.

c) New chemical processes caused by heavy ions.

Pulse radiolysis technique is one of the most powerful methods to investigate the primary processes. Fig.1 shows the concept of the pulse radiolysis technique. The initial short-lived species produced by pulsed ion beams can be detected by using time-resolved emission and absorption spectroscopes.

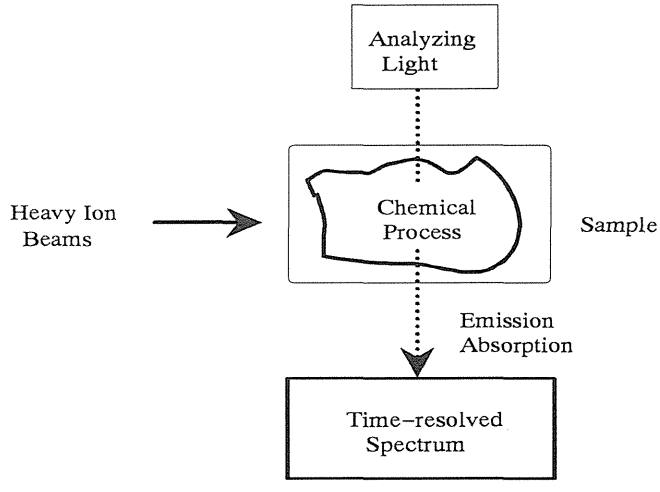

Fig. 1 The Principle of the heavy ion pulse radiolysis.

Recently, an effect of the high-densed excitation has been reported. Table 1 shows the difference of the fluorescence lifetimes from liquid n-dodecane irradiated by various kinds of radiation sources. The lifetimes decreased as increasing the values of LET. This result can be explained by the reaction of excited states of n-dodecane with reactive intermediates. In low LET irradiation, such as electron, the excited states cannot react with other intermediates, because they are isolated in the spur. In high LET irradiation, such as ion beams, the excited states are easily scavenged by the intermediates which densely produced in the track.

Table 1 Lifetimes of fluorescence from liquid n-dodecane by various kinds of radiation sources

Radiation Source	Energy [MeV]	LET [eV/Å]	Lifetime [ns]
Electron	28	0.02	4.3
Synchrotron Radiation	0.003~0.03	0.1~1	3.6
Ion (H^+)	2.9	1	3.2
Ion (H^+)	0.77	3	2.8
Ion (He^+)	1.9	15	2.3

In HIMAC, the shortest pulse width is presently longer than microseconds by using the beam course of the middle energy range after the injection linac. The plane to make a short pulse is expected. There are two effective methods to generate short pulse. One is a beam chopper after the acceleration section. The other is a bunching plate on the ion source. The bunching plate is better than the chopper in the view point of the strong intensity of the pulse. Anyway, the performance of the pulsed beam is very important for the elucidation of the primary processes.

References

H. Shibata, Y. Yosida S. Tagawa, Y. Aoki and H. Namba, Nucl Instrum. Meth., **A327**, 53 (1993).

Y. Aoki, N. Kouchi, H. Shibata, S. Tagawa, Y. Tabata and S. Imamura., Nucl Instrum. Meth., **B33**, 799 (1988).

Y. Yoshida, T. Ueda, T. Kobayashi, H. Shibata and S. Tagawa, Nucl Instrum. Meth., **A327**, 41 (1993).

N. Kouchi, Y. Aoki, H. Shibata, S. Tagawa, H. Kobayashi and Y. Tabata, Radiat. Phys. Chem., **34**, 759 (1989).

Y. Yoshida and S. Tagawa, "Dynamics and mechanisms of photoinduced transfer and related phenomena", ed. by N. Mataga, T. Okada and H. Masuhara, Elsevier, 435 (1992).

Y. Katsumura, Y. Yoshida, S. Tagawa and Y. Tabata, Radiat. Phys. Chem., **21**, 103 (1983).

A Project of
Microscopic Ion Beam Pulse Radiolysis of Aqueous Solutions

Y. Katsumura, D. Hiroishi, M. Domae and K. Ishigure
Department of Quantum Engineering and Systems Science
Faculty of Engineering, the University of Tokyo

A project of Microscopic Ion Beam Pulse Radiolysis of Aqueous Solutions has been proposed for one of the activities in the research field of radiation chemistry at HIMAC Facility. The aim of the study and experimental system will be discussed.

Introduction

It has been widely realized that understanding of the radiolysis of aqueous solution is a basic subject not only in the field of radiation chemistry but also many other fields which are closely related to radiation effect in science, technology, biology and medicine. As far as I know, a picture of the radiolysis of aqueous solution in diluted condition is well established and it can be said that we have enough knowledge from a practical view point[1]. Therefore the knowledge of the radiation chemistry in aqueous solution has been applied to the radiation effects in nuclear technology[2]. However, from the view points of concentration effect and LET effect in radiolysis of aqueous system we are still far from the complete. In the present paper, we propose a microscopic ion beam pulse radiolysis study of aqueous solution in the facility of HIMAC.

The aim of the project

Intensive work on the radiolysis of aqueous solution by using high energy ion beam had started more than four decades ago. It is easy to see the current state of the radiation chemistry of liquids and aqueous solutions by irradiation with heavy particles form a bibliography summarized by LaVern *et al.*, which covers papers appeared in 1901 up to 1988[3]. In spite of much work on the radiolysis of aqueous solution, most of the work employed a system of 0.4M sulfuric acid aqueous solution,

which is widely used as a Fricke and cerium dosimeters. Measurement of the $G(Fe^{3+})$ and $G(Ce^{3+})$ in the dosimeters can be described by using the yield of water decomposition products, $G_{e-aq} + G_H$, G_{OH}, G_{H2O2}.

$$G(Fe^{3+})_A = 3(G_{e-} + G_H) + G_{OH} + 2G_{H2O2} \quad (1)$$

$$G(Fe^{3+})_D = (G_{e-} + G_H) + G_{OH} + 2G_{H2O2} \quad (2)$$

$$G(Ce^{3+}) = (G_{e-} + G_H) - G_{OH} + 2G_{H2O2} \quad (3)$$

$$(G_{e-aq} + G_H) + 2G_{H2} = G_{OH} + 2G_{H2O2} = G_{-H2O} \quad (4)$$

where subscripts A and D indicate aerated and deaerated sample, respectively. By a combination of a mass balance relation, eq.(4), we calculate the values of $G_{e-aq} + G_H$, G_{OH}, G_{H2O2} and G_{H2} and G_{-H2O} are also obtainable. The G_{-H2O} is a value of net water decomposition. In 1961 Allen summarized the change of G-values of $G(Fe^{3+})_A$, $G(Fe^{3+})_D$ and $G(Ce^{3+})$ as a function of initial LET of heavy particles and showed the increase of molecular product with increasing the LET and, on the contrary, the decrease of radical products[4]. At the end of 1980s precise G-values of $G(Fe^{3+})_A$, $G(Fe^{3+})_D$ and $G(Ce^{3+})$ as a function of energy for each heavy particle have been presented by LaVerne and Schuler, which give the segmented yield of the $G(Fe^{3+})_A$, $G(Fe^{3+})_D$ and $G(Ce^{3+})$, and consequently, values of $G_{e-aq} + G_H$, G_{OH}, G_{H2O2} and G_{H2} and G_{-H2O} would be derived[5]. It is a surprising that there is only one set of data of G values for water decomposition in neutral pH as summarized in Table[6], in spite of the more close and important values for biological effects of radiation and radiation therapy than in acid solution. An interesting trend is that the G value of hydrated electron drops quickly with an increase of LET, which is confirmed by a recent experiment by irradiation with fast neutrons[7]. More or less, as a basic data, the determination of water decomposition product has been expected.

Table The G values of water decomposition products by irradiation with ion beams in neutral aqueous solution.

Radiation source	LET (eV/Å)	G_{H2}	G_H	G_{eaq-}	G_{OH}	G_{H2O2}	G_{-H2O}
Appleby&Schwarz (1969)							
18MeV D^+	(0.50)	0.68	0.64	1.48	1.66	0.91	3.48
32MeV He^{2+}	(2.3)	0.96	0.42	0.72	1.00	1.00	3.06
12MeV He^{2+}	(4.8)	1.11	0.27	0.42	0.75	1.08	2.91

It is known that ionizing radiation produces short lived transient species distributed locally along the flight path of the particle. This is so called spur and with increasing the density of the deposition energy separation between spurs are small and they are overlapped, which is cylindrical track. This picture is presented more than thirty years ago and simulation of the reactions based on the "diffusion kinetic model"[8] could explain the characteristics of the heavy ion irradiation. However, understanding of the microstructure of the spur or tracks is inevitably important to explain the experimental results and predict the reactions occurring in longer time ranges. In order to take the information of the structure of the tracks, a scavenging experiment is normally taken. The basic idea is that it can be observed the competition of the scavenging reaction with spur reactions, which can provide information of the structure and primary processes of the water radiolysis. This can be also applied to the theoretical work.

According to above mentioned, we have planned a project to determine the G values of water and concentration dependence of the yields of the primary species such as e^-_{aq}, H, and OH by using the pulse operation of HIMAC facility.

Experimental System

As a first step, we will take 24MeV He^{2+} pulse available in a room for medium energy experiment between the linear accelerator and the synclotron at HIMAC. A He^{2+} beam has a penetration depth of 0.4mm in aqueous solution. If we follow the change of absorbance as a function of position on the flight path in the solution, the yields of e^-_{aq}, H and OH would be obtainable as a function of LET. Since absorption coefficients of H atom and OH radical are not high in visible wavelength region, direct observations encounter several limitations and, thus, indirect methods in which the radicals are converted to another radicals with strong absorption bands in visible region would be taken. As for an analyzing light source, a He-Ne laser (633nm) will be used and, in future, a tunable laser would be convenient, which may allow us to broaden the target chemical species. At present, a resolution of less than 0.1 mm (100μm) is expected. A schematic diagram is shown in Fig. The components of the

system have been prepared and an experimental set-up will start at the end of January, 1994.

Fig. A schematic diagram of microscopic ion beam pulse radiolysis at HIMAC.

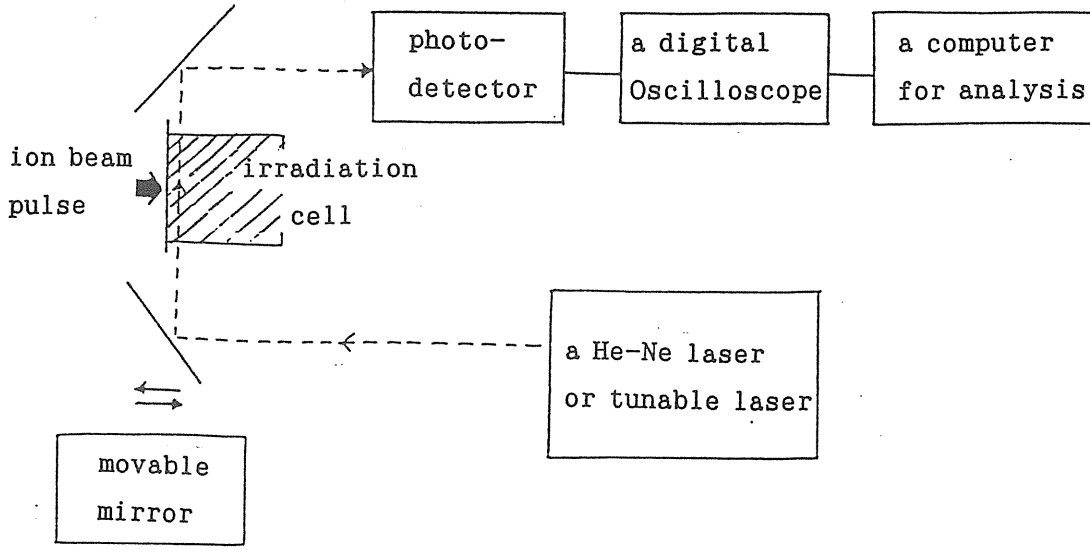

References

1) G. V. Buxton p.241-266 in *"The Study of Fast Processes and Transient Species by Electron Pulse radiolysis"*, NATO Advanced Study Institute Series C, Eds. by J. H. Baxendale and F. Busi, Reidel D. Publishing Company (1982)

2) B. V. Buxton, P.51-67 in *"New Trends and Developments in Radiation Chemistry"*, IAEA-TECDOC-527 (1989)

3) J. A. LaVerne, R. H. Schuler, A. B. Ross and W. P. Helman; *Radiat. Phys. Chem.* 17, 5-20 (1981). The updated bibliographic is available when requested to Dr. LaVerne.

4) A. O. Allen, *"The Radiation Chemistry of Water and Aqueous Solutions"*, Van Nostrand, New York, 1961.

5) J. A. LaVerne and R. H. Schuler; *J. Phys. Chem.*, **91**, 5770-5776 (1987), references cited herein.

6) A. Appleby and H.A. Schwarz; *J. Phys. Chem.*, 75, 1937-1941 (1969)

7) G. R. Sunaryo, Y. Katsumura, D. Hiroishi and K. Ishigure; *Radiat. Phys. Chem.* (1994) in press.

8) A. Kuppermann and G. G. Belford; *J. Chem. Phys.*, **36**, 1412-1426, 1427-1441 (1962)

Recent reports are summarized by J. A. LaVerne and S. M. Pimblott in *J. Chem. Soc. Faraday Trans.*, **89**, 3527-3532 (1993)

Secondary ions produced from gaseous and frozen targets under energetic (MeV/amu) heavy ion impact

T. Matsuo
Medical Research Institute,
Tokyo Medical and Dental University,
1-5-45 Yushima, Bunkyo-ku, Tokyo 113,

Abstract
Recent measurements of secondary ion production as a result of energetic heavy ion impact on gaseous and frozen targets are briefly reviewed. Relationship between these measurements and radiation chemistry and medicine is discussed.

It is well established that the production of recoil ions, especially that of multiply charged ions, is largely enhanced, when energetic heavy ions collide with atomic gaseous targets, compared with electron and light ion collisions[1]. In the past few years we investigated multiply-charged-ion production mechanisms in ~1 MeV/amu ion impact on molecular gas targets, and found efficient production of multiply charged atomic ions which are considered to be produced through rapid dissociation of molecular ions created by the primary energetic ion impact. It is also found that fragmented multiply charged atomic ions usually have large kinetic energies which are provided through Coulomb explosion of the multiply-charged molecular ions. Figure 1 shows the mass spectra of recoil ions produced in 1.05 MeV/amu-Ar^{12+} impact on gaseous H_2O. Peaks for multiply charged O^{i+} (i=2-6) ions as well as those for fragmented H^+, OH^+ and O^+ ions can be clearly seen.

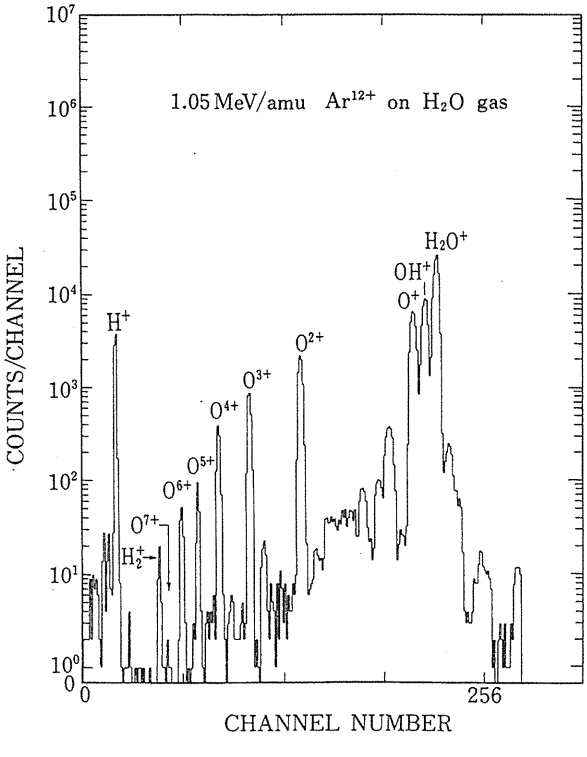

Recently, we have investigated production of secondary ions

from frozen gas surfaces under 1.5 MeV/amu-Ar^{13+} ion impact, and found that features of secondary ion production are quite different between gaseous and frozen targets[2,3]. The yields of multiply charged ions are sometimes strongly suppressed in the frozen targets, even though they are known to be copiously generated in the gaseous targets. For example, from the frozen surfaces of diatomic CO molecules, multiply-charged C^{i+} as well as O^{i+} ions (i=1-4) are efficiently produced, meanwhile the yields of multiply-charged C^{i+} ions are strongly suppressed in the frozen surfaces of triatomic CO_2 molecule. This result could be understood from the experimental fact that the carbon atom, located at the center of the CO_2 molecule, could not get kinetic energy sufficient to escape the surfaces through the Coulomb explosion of multiply-charged parent molecular ions (CO_2^{i+}) produced initially by the energetic ion impact[4]. It is also indicated that the frozen targets are efficient producers of molecular and cluster ions with various configurations.

Understanding the interaction of energetic ions with frozen surfaces are of importance from a fundamental view point of collision processes as well as from its practical implications in surface science, planetary science, bioscience and mass spectrometry. The present results of secondary ion production in gaseous targets are considered to be important in radiation chemistry and biology, as they are closely related to the primary events occurring in the heavy ion impact on living tissues. It has been postulated that high energy heavy ions cause a unique form of damages of living tissues; i.e., much higher lethal and oncogenic potentials compared with X-ray, electron and light ion irradiations. Moreover, DNA strand break caused by heavy ions is known to be more unreparable. In addition to the great ability of secondary electron production in heavy ion impact, the efficient production of fragmented ions, compared with those

in electron impact, might be responsible for the unique effects of heavy ion impact on living tissues. For further understanding the biological effect of heavy ion impact and its application to heavy ion therapy, collaboration of researchers in various areas would be necessary.

References

(1) C.L. Cocke and R.E. Olson, Phys. Rep. 205-No. 4, 155 (1991).
(2) H. Tawara, T. Tonuma, H. Kumagai, T. Matsuo and H. Shibata, J. Chem. Phys., 94, 2730 (1991).
(3) H. Tawara, T. Tonuma, H. Kumagai and T. Matsuo, Phys. Rev. A, 47, 1528 (1993).
(4) T. Matsuo, T. Tonuma, M. Kase, T. Kambara, H. Kumagai and H. Tawara, Chem. Phys., 121, 93 (1988).

---

* The present experiment was conducted at the RIKEN Heavy Ion Linear Accelerator Facility.